

Benzo[*a*]phenoxazinium-Based Red-Emitting Chemosensor for Zinc Ions in Biological Media

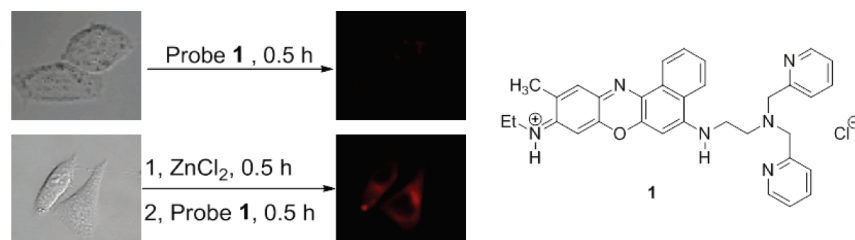
Xue-Bo Yang,[†] Bai-Xia Yang,[‡] Jian-Feng Ge,^{*,†} Yu-Jie Xu,[‡] Qing-Feng Xu,[†] Jie Liang,[†] and Jian-Mei Lu^{*,†}

Key Laboratory of Organic Synthesis of Jiangsu Province, College of Chemistry, Chemical Engineering and Material Science, Soochow University, 199 Ren' Ai Road, Suzhou 215123, China, and School of Radiation Medicine and Public Health, Soochow University, 199 Ren' Ai Road, Suzhou 215123, China.

lujm@suda.edu.cn; ge_jianfeng@hotmail.com

Received March 26, 2011

ABSTRACT



A benzo[*a*]phenoxazinium-based chemosensor bearing an *N,N*-di(2-picolyl)ethylenediamine unit was successfully synthesized. It is a long-wave emission and fully water-soluble fluorescent sensor with good membrane permeability for the selective detection of Zn²⁺.

Zinc is the second most abundant transition metal in the human body, since it is mostly trapped within proteins as a structural or catalytic cofactor,¹ and there is a pool of Zn²⁺ which is loosely bound or chelatable in the brain.² It is also known that disorder of Zn²⁺ metabolism is closely associated with many severe neurological diseases, including Alzheimer's disease (AD),³ cerebral ischemia,⁴ and epilepsy.⁵ Therefore, the measurement of Zn²⁺ is important in monitoring biological processes. For this purpose, several fluorescent Zn²⁺ sensors have been documented.^{6a–m} However, improvements are needed to overcome several limitations when they were applied to detect zinc in biological samples. First, most of reported sensors need to be excited by

UV light,^{6a–i} which can cause damage to living cells. Second, their fluorescence lies in the visible region,⁶ which cannot penetrate deep enough into human tissue. The sensor with long-wave absorption or emission region (650–900 nm) attracted much attention, since autofluorescence and photo-damage to living cells are reduced in this region.^{6n,o} However,

[†] Key Laboratory of Organic Synthesis of Jiangsu Province.

[‡] School of Radiation Medicine and Public Health.

(1) Berg, J. M.; Shi, Y. *Science* **1996**, *271*, 1081.
 (2) Frederickson, C. J. *Int. Rev. Neurobiol.* **1989**, *31*, 145.
 (3) Bush, A. I.; Pettingell, W. H.; Malthaup, G.; Paradis, M.; Vonsattel, J. P.; Gusella, J. F.; Beyreuther, K.; Masters, C. L.; Tanzi, R. E. *Science* **1994**, *265*, 1464.
 (4) Koh, J. Y.; Suh, S. W.; Gwag, B. J.; He, Y. Y.; Hsu, C. Y.; Choi, D. W. *Science* **1996**, *272*, 1013.
 (5) Frederickson, C. J.; Hernandez, M. D.; McGinty, J. F. *Brain Res.* **1989**, *480*, 317.

(6) (a) Maruyama, S.; Kikuchi, K.; Hirano, T.; Urano, Y.; Nagano, T. *J. Am. Chem. Soc.* **2002**, *124*, 10650. (b) Xu, Z.; Han, S. J.; Lee, C.; Yoon, J.; Spring, D. R. *Chem. Commun.* **2010**, *46*, 1679. (c) Hanaoka, K.; Muramatsu, Y.; Urano, Y.; Terai, T.; Nagano, T. *Chem.—Eur. J.* **2010**, *16*, 568. (d) Chen, H.; Gao, W.; Zhu, M.; Gao, H.; Xue, J.; Li, Y. *Chem. Commun.* **2010**, *46*, 8389. (e) Xue, L.; Liu, C.; Jiang, H. *Chem. Commun.* **2009**, 1061. (f) Aoki, S.; Sakurama, K.; Matsuo, N.; Yamada, Y.; Takasawa, R.; Tanuma, S.-i.; Shiro, M.; Takeda, K.; Kimura, E. *Chem.—Eur. J.* **2006**, *12*, 9066. (g) Komatsu, K.; Kikuchi, K.; Kojima, H.; Urano, Y.; Nagano, T. *J. Am. Chem. Soc.* **2005**, *127*, 10197. (h) Felton, C. E.; Harding, L. P.; Jones, J. E.; Kariuki, B. M.; Pope, S. J. A.; Rice, C. R. *Chem. Commun.* **2008**, 6185. (i) Zhang, L.; Dong, S.; Zhu, L. *Chem. Commun.* **2007**, 1891. (j) Komatsu, K.; Urano, Y.; Kojima, H.; Nagano, T. *J. Am. Chem. Soc.* **2007**, *129*, 13447. (k) Wong, B. A.; Friedle, S.; Lippard, S. J. *Inorg. Chem.* **2009**, *48*, 7009. (l) Qian, F.; Zhang, C.; Zhang, Y.; He, W.; Gao, X.; Hu, P.; Guo, Z. *J. Am. Chem. Soc.* **2009**, *131*, 1460. (m) Zhou, X.; Yu, B.; Guo, Y.; Tang, X.; Zhang, H.; Liu, W. *Inorg. Chem.* **2010**, *49*, 4002. (n) Guo, Z.; Zhu, W.; Zhu, M.; Wu, X.; Tian, H. *Chem.—Eur. J.* **2010**, *16*, 14424. (o) Peng, X.; Wu, T.; Fan, J.; Wang, J.; Zhang, S.; Song, F.; Sun, S. *Angew. Chem., Int. Ed.* **2011**, *50*, 4180.

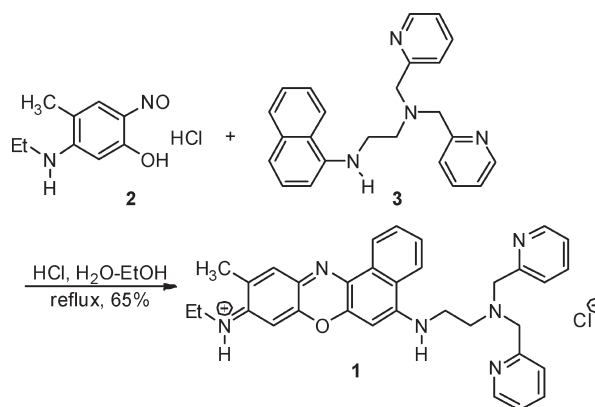
cases of Zn^{2+} sensors in the long-wave fluorescent emission are still less common.⁷ Only two of them, which worked in organic cosolvent required conditions, could be used in imaging in biological systems.^{7a,b} And there is no report on a full water-soluble long-wave fluorescence probe for imaging zinc in biological samples. In this regard, it is highly desirable to develop Zn^{2+} -selective full water-soluble long-wave fluorescent sensors to match harmless imaging and visualization of Zn^{2+} in living cells.

Benzo[*a*]phenoxazinium derivatives have absorption bands in the 580–610⁸ or 629–632 nm⁹ region, and the corresponding emission bands are between 650 and 670 nm in water.^{8,9} They have good membrane permeability and comparatively low toxicity according to in vitro and in vivo assay results,^{10a,b} and a red-emitting phenoxazinium based probe, 3-(diethylamino)-7-(1,4-dioxo-7,13-dithia-10-azacyclopentadecan-10-yl)phenoxazin-5-ium chloride, has been reported as a low-cost and real-time monitoring probe for selective ratiometric detection of Hg^{2+} in pure water.^{10c} Therefore, we have focused on the synthesis of a new sensor based on the benzo[*a*]phenoxazinium skeleton and investigated its chemodosimetric properties that can provide sensitive measurement of the Zn^{2+} in a 100% aqueous environment. Compound **1** exhibits an absorption peak at 582 nm and has the maximal emission bands at 656 nm with a high quantum yield in PBS buffer. More importantly, the chloride salt shows an excellent solubility and intense fluorescence, even in aqueous media. In addition, for demonstration of its application in biological samples, the application of **1** to cultured KB human oral epidermoid carcinoma cell (KB cell) were implemented and discussed.

As depicted in Scheme 1, the benzo[*a*]phenoxazinium derivative (**1**) was prepared in 65% yield from the reaction of 5-(ethylamino)-4-methyl-2-nitrosophenol (**2**) with naphthalene derivative (**3**) in acidic ethanol solution. The identities of all synthetic compounds were fully confirmed by ¹H NMR, ¹³C NMR, and mass spectroscopy. All photochemical experiments were carried out in PBS buffer at pH 7.4 without any organic cosolvent.

Figure 1 shows the changes in the absorption spectrum of **1** as a function of Zn^{2+} concentration at room temperature. The UV–vis spectrum of **1** is characterized by two absorption maxima at 582 nm ($\epsilon = 35000 \text{ M}^{-1} \cdot \text{cm}^{-1}$) and 623 nm ($\epsilon = 25000 \text{ M}^{-1} \cdot \text{cm}^{-1}$). These are responsible for

Scheme 1. Synthesis of Benzo[*a*]phenoxazinium **1**



the light blue color of the solution. During photometric titrations of **1** with Zn^{2+} , the absorption wavelength at 582 nm was slightly changed, and there was gradually decrease of absorption at 623 nm. These may be induced by the changes of the molecular orbitals resulting of the complexation of Zn^{2+} with the *N,N*-di(2-picolyl)ethylenediamine (DPEN) unit.

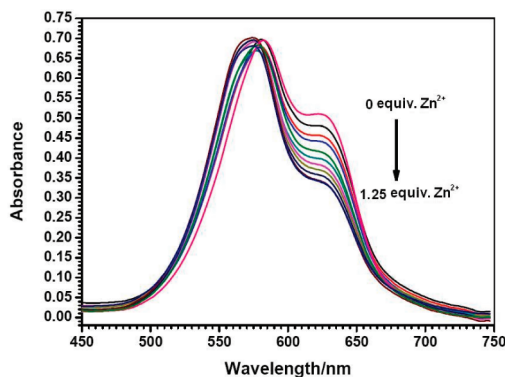


Figure 1. Changes in the UV–vis spectra of **1** ($20 \times 10^{-6} \text{ M}$ in PBS buffer, pH = 7.4) upon titration by ZnCl_2 from $1.5 \times 10^{-6} \text{ M}$ to $25 \times 10^{-6} \text{ M}$.

According to the linear Benesi–Hildebrand expression,¹¹ the measured absorbance $[1/(A - A_0)]$ at 623 nm shows a linear relationship with a change of $1/[\text{Zn}^{2+}]$ ($R = 0.994$), indicating the 1:1 stoichiometry between Zn^{2+} and **1** (Figure 2 and Figure S3, Supporting Information). The job plot analysis¹² of the UV–vis titrations carried out in water revealed a maximum of 50% mole fraction in accordance with the proposed 1:1 binding stoichiometry (Figure S1, Supporting Information). On the basis of the 1:1 stoichiometry and UV–vis titration

(7) (a) Lu, X.; Zhu, W.; Xie, Y.; Li, X.; Gao, Y.; Li, F.; Tian, H. *Chem.—Eur. J.* **2010**, *16*, 8355. (b) Tang, B.; Huang, H.; Xu, K.; Tong, L.; Yang, G.; Liu, X.; An, L. *Chem. Commun.* **2006**, 3609. (c) Atilgan, S.; Ozdemir, T.; Akkaya, E. U. *Org. Lett.* **2008**, *10*, 4065. (d) Hung, C.-H.; Chang, G.-F.; Kumar, A.; Lin, G.-F.; Luo, L.-Y.; Ching, W.-M.; Wei-Guang Diao, E. *Chem. Commun.* **2008**, 978. (e) Kiyose, K.; Kojima, H.; Urano, Y.; Nagano, T. *J. Am. Chem. Soc.* **2006**, *128*, 6548.

(8) (a) Frade, V. H. J.; Gonçalves, M. S. T.; Moura, J. C. V. P. *Tetrahedron Lett.* **2006**, *47*, 8567. (b) Lee, M. H.; Lee, S. W.; Kim, S. H.; Kang, C.; Kim, J. S. *Org. Lett.* **2009**, *11*, 2101.

(9) Jose, J.; Ueno, Y.; Burgess, K. *Chem.—Eur. J.* **2009**, *15*, 418.

(10) (a) Ge, J. F.; Arai, C.; Yang, M.; Md., A. B.; Lu, J.; Ismail, N. S. M.; Wittlin, S.; Kaiser, M.; Brun, R.; Charman, S. A.; Nguyen, T.; Morizzi, J.; Itoh, I.; Ihara, M. *ACS Med. Chem. Lett.* **2010**, *1*, 360. (b) Ihara, M. *Heterocycles* 201110.3987/REV-11-706. (c) Yang, X. B.; Ge, J. F.; Xu, Q. F.; Zhu, X. L.; Li, N. J.; Gu, H. W.; Lu, J. M. *Tetrahedron Lett.* **2011**, *52*, 2492.

(11) Zhu, M.; Yuan, M. J.; Liu, X. F.; Xu, J. L.; Lv, J.; Huang, C. S.; Liu, H. B.; Li, Y. L.; Wang, S.; Zhu, D. B. *Org. Lett.* **2008**, *10*, 1481.

(12) Zhou, Y.; Wang, F.; Kim, Y.; Kim, S.-J.; Yoon, J. *Org. Lett.* **2009**, *11*, 4442.

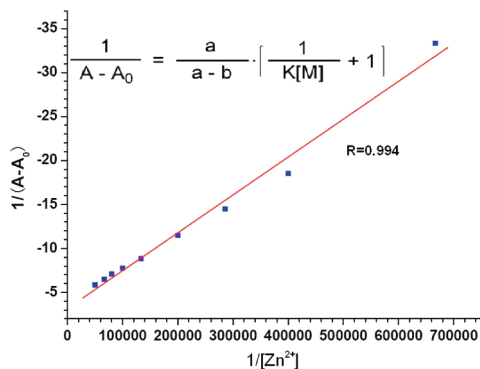


Figure 2. Benesi–Hilderbrand plot of **1** with Zn^{2+} .

data in Figure 1, the association constant of **1** with Zn^{2+} in water was found to be $7.35 \pm 0.90 \times 10^4 \text{ M}^{-1}$.

The fluorescence titration of **1** ($20 \times 10^{-6} \text{ M}$) in the presence of different Zn^{2+} concentrations was also performed. As shown in Figure 3, sensor **1** showed a fluorescence emission at 656 nm ($\Phi_f = 0.15$). Upon increasing the concentration of Zn^{2+} to $25 \times 10^{-6} \text{ M}$, the emission intensity at 656 nm gradually increased ($\Phi_f = 0.28$, Table S1, Supporting Information). The fluorescent probe **1** ($20 \times 10^{-6} \text{ M}$) can detect the concentration of Zn^{2+} from 1.5×10^{-6} to $20 \times 10^{-6} \text{ M}$ (Figure 3 Inset) in PBS buffer (pH = 7.4). At the employed concentration of the probe ($20 \times 10^{-6} \text{ M}$), the limit of detection for Zn^{2+} is $1.5 \times 10^{-6} \text{ M}$ (Figure 3 inset). The excitation and emission spectra are shown in Figure S4, Supporting Information.

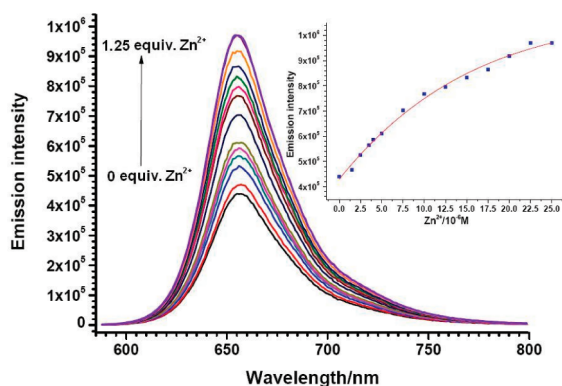


Figure 3. Emission spectra of compound **1** in the presence of an increasing Zn^{2+} concentration (from 1.5×10^{-6} to $25 \times 10^{-6} \text{ M}$) in PBS buffer (pH = 7.4). The excitation wavelength was 579 nm with 5 nm slit widths. The concentration of chemosensor **1** was $20 \times 10^{-6} \text{ M}$. Inset: Fluorescence intensity of **1** versus the Zn^{2+} concentration at 656 nm.

To evaluate the selectivity of the fluorescent probe **1** toward Zn^{2+} ions, competition experiments were performed. As shown in Figure 4, only some of the other cations interfere with the fluorimetric analysis of Zn^{2+} .

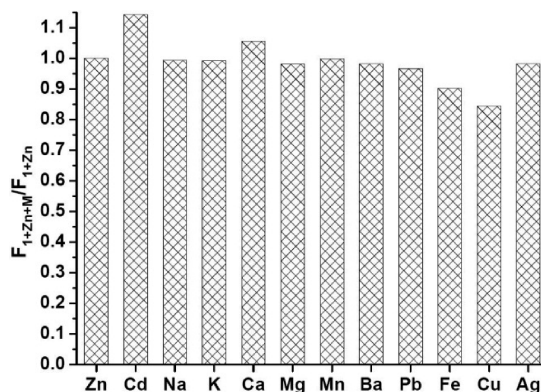


Figure 4. Fluorescence response of **1** ($20 \times 10^{-6} \text{ M}$) containing $20 \times 10^{-6} \text{ M}$ Zn^{2+} to the selected metal ions ($20 \times 10^{-6} \text{ M}$: Cd^{2+} , Cu^{2+} , Pb^{2+} , Fe^{3+} , Ag^+ , Ba^{2+} , Mn^{2+} ; $100 \times 10^{-3} \text{ M}$: K^+ , Na^+ , Mg^{2+} , Ca^{2+}) in PBS buffer (pH = 7.4). $F_{1+\text{Zn}}$ indicates the fluorescence signals of **1** in the presence of Zn^{2+} and $F_{1+\text{Zn}+\text{M}}$ denotes the fluorescence signals of **1** in the presence of Zn^{2+} and competing ions. Excitation was at 579 nm and emission was at 656 nm.

The titration of Zn^{2+} to **1** in the presence of the screened metal cations (K^+ , Na^+ , Mg^{2+} , Pb^{2+} , Ag^+ , Ba^{2+} , and Mn^{2+}) did not lead to any changes to the fluorescence output. Cd^{2+} and Ca^{2+} enhanced the fluorescence intensity, and some paramagnetic metal ions, such as Fe^{3+} and Cu^{2+} , slightly quench the fluorescence.

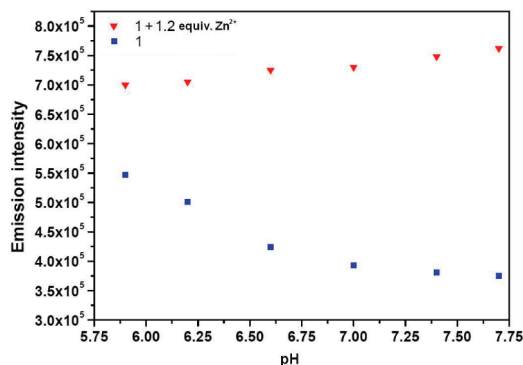


Figure 5. The fluorescence intensity of compound **1** ($20 \times 10^{-6} \text{ M}$) in the absence (■) and in the presence (▼) of Zn^{2+} ($24 \times 10^{-6} \text{ M}$) at different pH values in a phosphate buffer ($100 \times 10^{-3} \text{ M}$); $\lambda_{\text{ex}} = 579 \text{ nm}$, $\lambda_{\text{em}} = 656 \text{ nm}$.

The fluorescence intensity changes at 656 nm at a pH ranging from 5.90 to 7.70 are shown in Figure 5. The fluorescence intensity of **1** was slight enhanced with the increase of pH value, and the situation was opposite on the mixed solution of **1** and Zn^{2+} . The differentials of emission intensity around pH ~ 7.4 did not have a large variation, which means **1** can be used to analyze intracellular Zn^{2+} ions in biological samples.

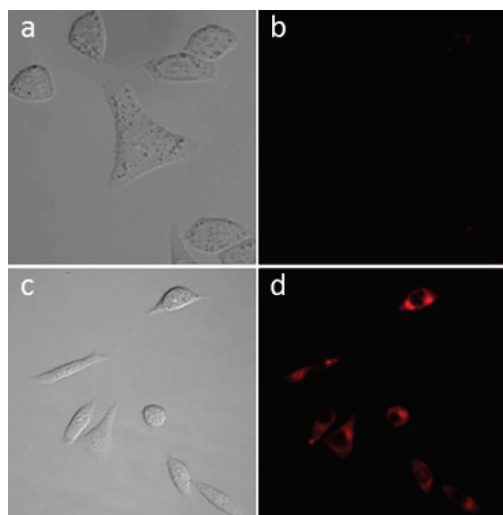


Figure 6. Confocal fluorescence images in KB cells. Top (a, b): Cells incubated with **1** (20×10^{-6} M) for 0.5 h. Bottom (c, d): Cells incubated with ZnCl_2 (100×10^{-6} M) for 0.5 h and washed with PBS, then **1** (20×10^{-6} M) for 0.5 h. Emission was collected at 520 – 620 nm upon excitation at 514 nm. Bright field (a and c) fluorescence (b and d).

The application of **1** on the cultured cells was checked. Bright-field measurements confirmed that the cells after treatment with Zn^{2+} and **1** were viable throughout the imaging experiments (Figure 6a and 6c). Under selective excitation of **1**, staining KB cells with a 20×10^{-6} M solution of **1** for 30 min at 37°C led to very weak intracellular fluorescence (Figure 6b). After the cells were supplemented with ZnCl_2 (20×10^{-6} M) for 30 min at 37°C and washed with PBS, then loaded with **1** under the same conditions, a significant increase in the fluorescence from the intracellular area was observed (Figure 6d). These results suggested that **1** has good membrane permeability and can be used to monitor changes in intracellular Zn^{2+} . It can be useful in clarifying the intracellular concentration of Zn^{2+} in biological systems.

In addition, the MTT assay was used to investigate the cytotoxicity of **1** to the KB cell (Figures S5, Supporting Information). The cell viability is about 89–109%, which was obtained by the percentage of KB cell viability remaining after cell treatment with **1** (untreated cells were considered to have 100% survival) between 10×10^{-6} and 30×10^{-6} M, and the damage of MTT for the cells will be reduced by the protecting from compound **1** at 20×10^{-6} M concentration. The result indicated the probe **1** has no obvious cytotoxicity in the concentration region, and **1** can be a suitable fluorescence chemosensing probe for the detection of Zn^{2+} in biological systems.

In conclusion, this study presents an example of the selection of a suitable fluorophore for zinc ion probes from existing or potential drug molecules. A benzo[*a*]-phenoxazinium-based chemosensor bearing an *N,N*-di-(2-picolyl)ethylenediamine unit (**1**) was used as a promising analytical tool for detecting fluorometric zinc ions with long-wave emission. Specifically, this probe is one of the few red-emitting fluorescent probes that allows for the selective detection of zinc ions in PBS buffer with no organic cosolvent required. Notably, the selectivity of the probe for Zn^{2+} over other metal ions is extremely high. In the sense of long-wave excitation/emission, water solubility, low cytotoxicity, and membrane permeability nature, **1** can be one of the most promising probes for the detection of Zn^{2+} in water and in living cells.

Acknowledgment. We are grateful to Professor Masataka Ihara (Hoshi University, Japan) for the helpful discussion regarding the synthesis of **1**. The project is financially supported by the National Environmental Community Project of China (200909044), Natural Science Fund (BK2009113), and Natural Science Fund for Colleges and Universities (08KJB430013) in Jiangsu Province.

Supporting Information Available. Synthesis; characterization of **1**; KB cell culture MTT assay. This material is available free of charge via the Internet at <http://pubs.acs.org>